Comfort Properties of PLA/cotton Multilayered Quilted Fabrics

Zixin Ju[1], Shanshan Dong[1], Winghei Lau[1], Yanping Liu[2], Hong Hu[1,*]

[1]School of Fashion and Textiles, The Hong Kong Polytechnic University, Hung Hom, Kowloon, Hong Kong.

[2]College of Textiles, Donghua University, Songjiang District, Shanghai

21118991r@connect.polyu.hk; 21119051r@connect.polyu.hk; winghei.lau@polyu.edu.hk; liuyp@dhu.edu.cn; hu.hong@polyu.edu.hk

[*]Corresponding author: hu.hong@polyu.edu.hk; Tel.: +852-3400-3089

Abstract

This paper reported a study on the comfort properties of poly(lactic acid) (PLA)/cotton multilayered quilted fabrics. Fifteen multilayered quilted fabrics with diverse structural parameters were first fabricated using three different linear densities of PLA filaments as inlaid yarns and five distinct blending ratios of PLA/cotton blended yarns as surface yarns. Then, their comfort properties, including air permeability, water vapor permeability, and thermal and compressive properties, were tested. The effects of the inlaid yarns' linear density and surface yarns' blending ratio on these properties were systematically analyzed, and multiple regression models were established to accurately describe these relationships, with all correlation coefficients exceeding 0.97. Based on this, a multi-objective optimization model was developed, and optimization calculations were performed using the MATLAB genetic algorithm tool to determine the optimal yarn parameters for enhancing overall comfort performance. The results indicated that selecting 450D PLA for the inlaid yarn and a 50/50 PLA/cotton blend for the surface yarn achieved superior overall comfort properties, along with enhanced air and moisture permeability. To improve thermal and compressive properties, it was recommended to use inlaid 900D PLA and surface 100% PLA yarns. Furthermore, these optimized fabrics exhibited excellent dimensional stability and tensile properties even after undergoing 20 washes, proving their durability. This study will promote PLA application in textiles and provide valuable insights for designing eco-friendly quilted fabrics.

Keywords: PLA filaments; PLA/cotton blended yarn; multilayered quilted fabrics; comfort property; thermal-physiological property; compressive property

1. Introduction

It is widely recognized that the majority of synthetic polymers originate from non-renewable petroleum sources and exhibit slow degradation in landfills, contributing to air pollution, groundwater contamination, and global warming.[1] As global environmental awareness rises, there is a growing trend towards developing high-performance, eco-friendly products derived from natural resources.[2] Poly(lactic acid) (PLA), derived from renewable sources such as corn, sugar beets, wheat starch, and potatoes,[3] is the only biobased and biodegradable polymer that can be extensively melt-spun into textile fibers, making it a unique and attractive choice for developing sustainable products.[4] PLA is fully compostable at the end of its lifecycle, further enhancing its appeal among environmental advocates.[5] Furthermore, PLA has gained considerable attention within the textile industry for its exceptional moisture conductivity, flame-retardant, antimicrobial, UV-resistant, and other beneficial textile properties.[4] However, PLA faces challenges such as lower moisture regain and thermal stability, which restrict its textile applications.[4]

To address the limitations of PLA, researchers have explored blending it with other fibers such as lyocell,[6] flax,[7] modal,[8] wool,[9] and cotton[3,10] to combine their complementary strengths and enhance overall performance. Among these materials, cotton stands out as a particularly promising option for blending with PLA due to its environmental friendliness and cost-effectiveness. Previous studies have primarily investigated the spinning parameters of PLA/cotton blended yarns,[10] along with research on the pretreatment and dyeing processes of PLA/cotton blended fabrics,[11-13] and limited exploration into the moisture and thermal properties of these fabrics.[3] On the other hand, the existing studies on PLA/cotton blended fabrics mainly focus on single-layer structures and investigations into related multilayer fabrics such as weft knitted quilted fabrics still lack.

Weft knitted quilted fabric, a special type of multilayered fabric, consists of an upper, middle, and lower layer. The upper and lower layers in quilted fabrics are connected through tuck or loop stitches during production, while the middle layer is characterized by the insertion of non-knitted inlaid yarns.[14,15] The usage of inlaid yarns generates additional air layers in the non-quilted areas, thereby enhancing the fabric's bulkiness and thermal insulation. Furthermore, distinct fiber materials can be selectively employed in each of the three layers of quilted fabrics to attain the desired

performance.[14] Owing to their exceptional shape retention, variable patterns, adjustable weight and thickness, and enhanced thermal capacity, quilted fabrics are widely applicable in winter apparel, sleeping bags, automotive seats, as well as bedding and furniture covers.[14] Consequently, the investigation of sustainable multilayered quilted fabrics holds considerable importance.

In addition to being eco-friendly, a competent quilted fabric should possess excellent comfort properties, as fabric comfort is one of the most pivotal factors influencing fabric selection.[16] Comfort refers to the physiological sensations experienced by the human body when wearing or interacting with a fabric, and it is primarily determined by the combined effect of thermal-physiological and sensorial comfort.[17] Thermo-physiological comfort, governed by the transport of airflow, moisture, and heat through the fabric, can be assessed through parameters such as air permeability, water vapor permeability, thermal conductivity, thermal resistance, and heat retention property.[18,19] Sensorial comfort depends on the fabric surface and mechanical properties, often evaluated through compressive testing. Compressive property is extremely significant, particularly for multilayered fabrics, as it significantly influences fabric handles, including softness, fullness, and surface smoothness.[18,20] These comfort attributes are mainly influenced by fabric structural parameters such as weight, thickness, density, porosity, and material compositions.[21,22] Therefore, such factors should be thoroughly considered in the design of quilted fabrics.

To date, a research gap still exists in the comprehensive investigation of comfort properties of sustainable multilayered quilted fabrics made from PLA filaments and PLA/cotton blended yarns. To fill this research gap, the present study fabricated fifteen multilayered quilted fabrics with varied structural parameters. This was achieved by using three different linear densities of PLA filaments as inlaid yarns in the middle layer and five distinct blending ratios of PLA/cotton blended yarns as surface yarns in the upper and lower layers. It is noteworthy that all the employed yarns are sustainable and suitable for large-scale production of multilayered quilted fabrics efficiently by using weft circular knitting technology in just one single process. This work systematically studies the effects of linear density of inlaid PLA filaments and the blending ratio of surface PLA/cotton blended yarns on the comfort properties of multilayered quilted fabrics, including air permeability, water vapor permeability, and thermal and compressive properties. Multiple regression analysis is conducted to establish precise

mathematical models that can be used to describe the relationships between each comport property and yarn parameters. Moreover, the study also seeks to develop a multi-objective optimization model and utilize genetic algorithms to identify optimal yarn parameters for improved overall performance of the quilted fabrics. Furthermore, durability in terms of dimensional stability and tensile properties is also assessed for the optimized fabrics after repeated washing cycles.

2. Materials and methods

2.1 Materials

The multilayer quilted fabrics developed in this study consist of an upper layer, a middle layer, and a lower layer, with a careful selection of biodegradable PLA filaments as inlaid yarns in the middle layer. This selection is based on the consideration of current environmental concerns. The PLA filaments used were sourced from Qingdao Ruomi Technology Co., Ltd., with linear densities of 450D, 600D, and 900D. Detailed technical information of these PLA filaments is listed in Table 1, including yarn linear density measured following ASTM D1907-01 and tensile properties (tenacity and elongation) tested according to ASTM D2256.[23,24] Table 1 demonstrates that the thicker 900D PLA filament exhibits a lower tenacity of 17.83 cN/tex. This phenomenon arises because all PLA inlaid filaments were merged from multiple 150D PLA filaments, indicating that the thicker 900D filament consists of a greater number of finer PLA filaments. Consequently, during the tensile test, these finer filaments in the 900D PLA filament were more prone to break at different points, leading to reduced tenacity.

Table 1. The technical details of inlaid PLA filaments used

Yarn	Linear density (Denier)	Tenacity (cN/tex)	Elongation (%)
450D PLA	458.15 (± 1.45)	19.41 (± 1.17)	24.16 (± 0.99)
600D PLA	609.75 (± 0.31)	19.53 (± 0.95)	22.17 (± 0.91)
900D PLA	905.18 (± 1.34)	17.83 (± 0.96)	23.07 (± 0.99)

Note: The values enclosed within parentheses correspond to the standard deviations.

Meanwhile, five types of PLA/cotton blended yarns, with the same English yarn count (32 Ne), but with different ratios (100% PLA, 100% cotton, PLA/cotton 70:30, 50:50,

and 30:70), were used as surface yarns for both the upper and lower layers of the quilted fabrics. A portion of the blended yarns in the lower layers simultaneously served as connecting yarns to link these separate layers. These staple yarns were acquired from the Quanzhou Smartwin International Group Co., Ltd. The technical details and morphological characteristics of these staple yarns are presented in Table 2 and Table 3, respectively. Yarn count and tensile properties were evaluated similarly to the PLA filaments described above,[23,24] while yarn hairiness, unevenness, and twist were measured according to ASTM D5647-07,[25] ASTM D1425,[26] and ASTM D1422,[27] respectively. From Table 2, it is found that, despite maintaining similar yarn counts and twists across different blended yarns, notable differences were observed in tenacity, elongation, unevenness, and hairiness. These variations primarily stem from inherent disparities between cotton and PLA fibers. Cotton fibers, being natural, are prone to containing neps, short fibers, and impurities, thereby increasing yarn unevenness and hairiness while reducing tenacity and elongation at break.[28] Conversely, 100% PLA filaments exhibit lower unevenness (6.96%) and hairiness (4.75), along with higher tenacity (13.85 cN/tex) and elongation (6.71%). Additionally, the properties of blended yarns do not exhibit a linear change with the blending ratio, highlighting the diverse and complex factors influencing their performance. Factors such as fiber interaction, binding force, and uniform distribution within a blended yarn collectively impact its final properties.

Table 2. The technical details of staple yarns used

Yarn	Yarn count (Ne)	Tenacity (cN/tex)	Elongation (%)	Unevenness (%)	Hairiness (H)	Twist (per inch)
100% PLA	31.62 (± 0.14)	13.85 (± 0.50)	6.71 (± 0.38)	6.96 (± 0.05)	4.75 (± 0.18)	19.80 (± 0.39)
70% PLA 30% cotton	31.50 (± 0.37)	10.30 (± 0.37)	7.10 (± 0.33)	9.87 (± 0.05)	2.87 (± 0.03)	20.26 (± 0.35)
50% PLA 50% cotton	31.63 (± 0.12)	10.59 (± 0.35)	5.93 (± 0.60)	12.89 (± 0.15)	3.98 (± 0.11)	20.06 (± 0.35)
30% PLA 70% cotton	31.51 (± 0.25)	12.59 (± 0.39)	6.17 (± 0.17)	8.29 (± 0.08)	3.32 (± 0.08)	19.87 (± 0.43)
100% cotton	31.79 (± 0.54)	12.11 (± 0.64)	5.24 (± 0.15)	11.54 (± 0.10)	5.68 (± 0.05)	20.40 (± 0.51)

Note: The values enclosed within parentheses correspond to the standard deviations.

Table 3. The morphologies of staple yarns used

Yarn	Longitudinal morphology	Cross-sectional morphology
100% PLA	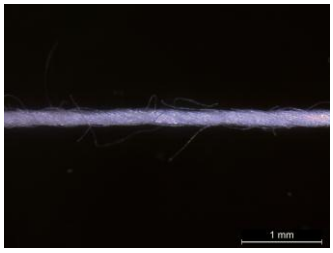	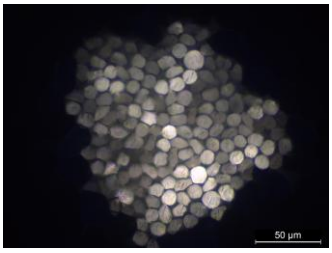
70% PLA 30% cotton	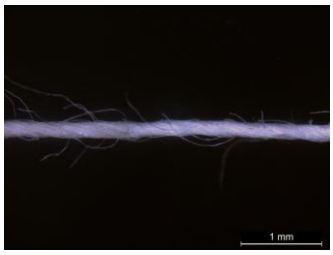	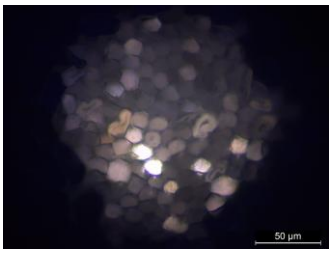
50% PLA 50% cotton		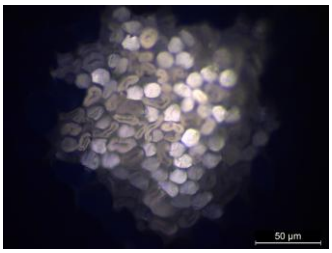
30% PLA 70% cotton	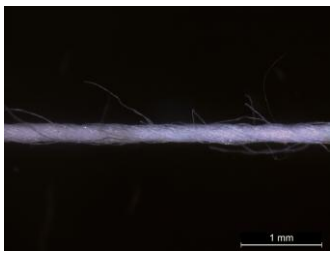	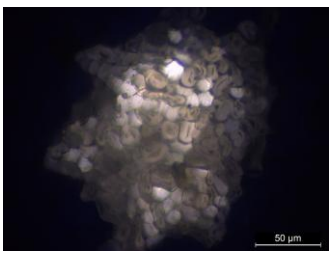
100% cotton	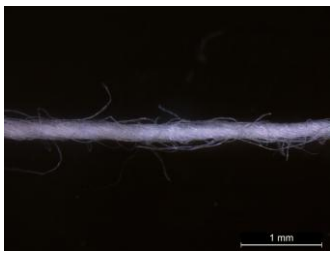	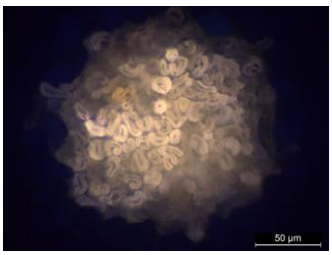

2.2 Fabric production

Fifteen types of multilayered quilted fabrics were produced on an electronic double jacquard circular knitting machine (TERROT UCC548) with a 30-inch diameter, 22-gauge, 48 yarn feeders, and a total number of 4104 needles. As shown in Figure 1(a), the designed pattern was initially generated by Autopaint software on a computer and subsequently sent to the circular machine (Figure 1(b)) for production. It is important to note that consistent knitting patterns and parameters such as yarn input tension, fabric

take-down tension, and cam setting were employed for all fabrics in this study. The knitting process is shown in Figure 1(c), where 6 feeders were required to complete a knitting cycle. While the inlaid PLA filaments were fed into between the cylinder and dial needles by the 1st and 4th feeders without loop formation during the knitting process, the staple yarns were fed to the cylinder needles, dial needles, or both cylinder and dial needles by the 2nd, 3rd, 5th and 6th feeders to form only face loops, only back loops or both face and back loops, respectively. The connection between the upper and lower layers of the fabric was created due to the simultaneous formation of the face and back loops at the 2nd feeder by selecting specific cylinder needles according to the designed pattern. Figure 1(d) schematically shows the structure of the quilted fabric, while Figures 1(e)-(g) provide corresponding actual images. Further production details for all fabrics are presented in Table 4.

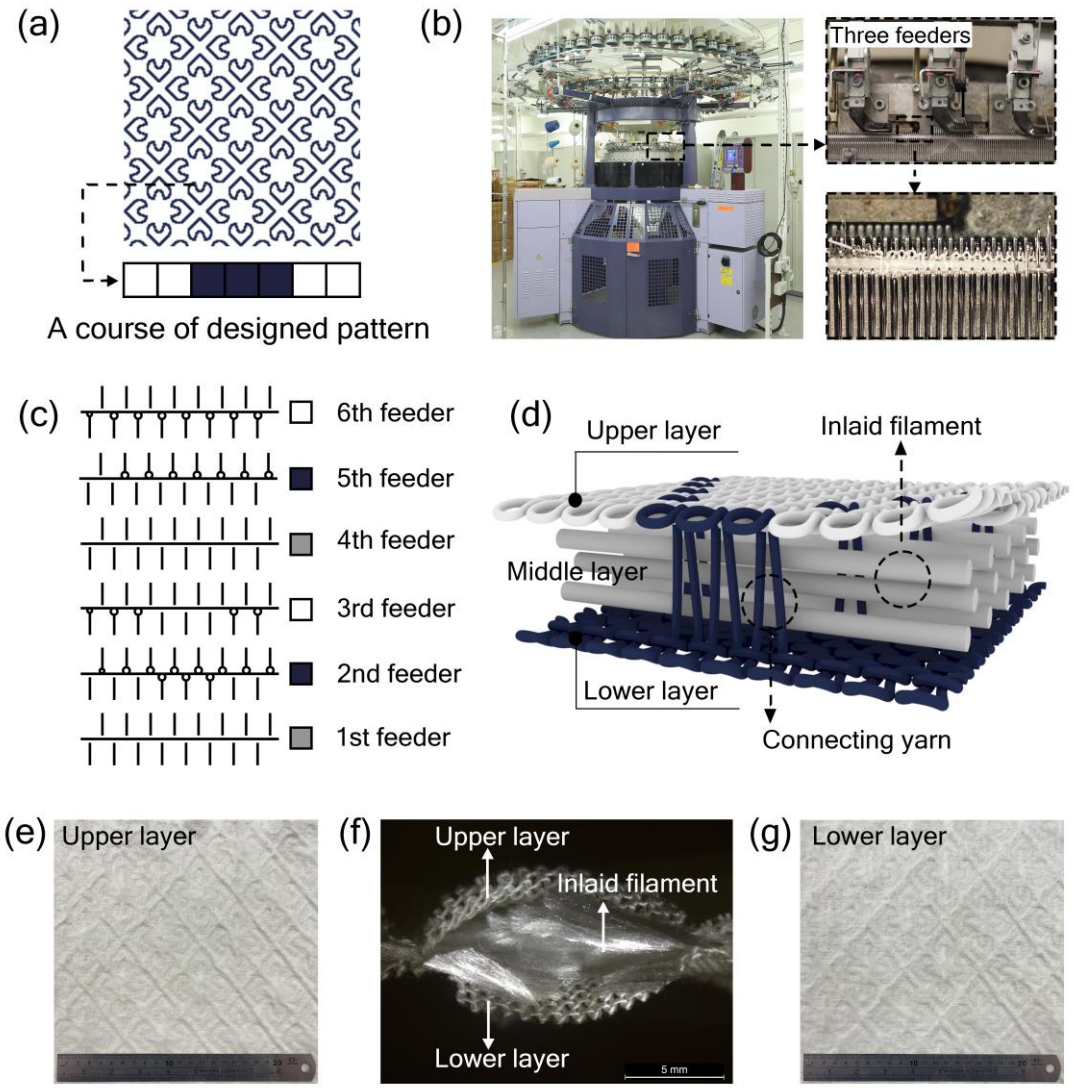

Figure 1. The knitting process and images of quilted fabric: (a) the designed pattern;

(b) the circular knitting machine used; (c) the knitting process; (d) the schematic illustration of fabric structure; (e) image of the fabric upper layer; (f) image of the cross-section; (g) image of the fabric lower layer.

Table 4. Production details of all quilted fabrics

Sample no.	Yarns for surface layers	Inlaid yarns
1	100% PLA	450D PLA filament
2	70% PLA 30% cotton	450D PLA filament
3	50% PLA 50% cotton	450D PLA filament
4	30% PLA 70% cotton	450D PLA filament
5	100% cotton	450D PLA filament
6	100% PLA	600D PLA filament
7	70% PLA 30% cotton	600D PLA filament
8	50% PLA 50% cotton	600D PLA filament
9	30% PLA 70% cotton	600D PLA filament
10	100% cotton	600D PLA filament
11	100% PLA	900D PLA filament
12	70% PLA 30% cotton	900D PLA filament
13	50% PLA 50% cotton	900D PLA filament
14	30% PLA 70% cotton	900D PLA filament
15	100% cotton	900D PLA filament

2.3 Experiment

After fabric production, all fabric specimens were subjected to an initial washing and subsequent drying procedure according to ISO 6330 standard.[29] These processes were aimed to effectively eliminate the water-soluble impurities and reduce the dimensional instability of the fabrics. Prior to any characterization and testing, the fabric samples were relaxed and conditioned for 24 hours under the standard atmospheric conditions (20 ± 2°C and 65 ± 2% relative humidity) as specified by ISO 139 standard.[30] The comfort properties of the produced multilayered quilted fabrics, including air permeability, water vapor permeability, thermal and compressive properties, were then evaluated.

2.3.1 Physical properties

The morphologies of staple yarns and quilted fabrics were observed using LEICA DM2700 M and LEICA M165C optical microscopes, respectively. The grams per square meter (GSM) of the fabric samples was determined according to standard ASTM D3776-09 using the SHIMADZU BX 300 electronic balance.[31] Fabric thickness measurements were conducted by means of the RME5 thickness tester in accordance with standard ASTM D1777-96.[32] Fabric stitch densities were determined by counting the wales and courses per unit length of the upper fabric layer, following ASTM D3887-96 guidelines and employing a counting glass.[33] Fabric surface porosity was evaluated using image processing technology. Images of fabric samples were captured at 1.6x magnification with a LEICA DM2700 M microscope. These images were converted to binary format in Adobe Photoshop 2023, where black pixels represented pores and white pixels represented yarns. MATLAB R2023a (The MathWorks, Natick, USA) was then used to calculate porosity by determining the black to total pixels ratio.

2.3.2 Air permeability

Air permeability was assessed using the KES (Kawabata Evaluation Systems)-F8-AP1 Air Permeability Tester, in which a consistent airflow was generated through a plunger/cylinder mechanism. The air passed through the specimen and into the environment, allowing the quantification of air pressure loss attributed to the specimen's air resistance, expressed in kPa·s/m. Each air permeability test was performed on a 12 cm × 12 cm fabric sample, with five samples prepared for each fabric type.

2.3.3 Water vapor transmission rate

The water vapor transmission rate (WVTR) test was performed following the British Standard 7209,[34] using a SDL Atlas M261 water vapor permeability tester. In this procedure, a specific volume of water was transferred into an open test dish. Then, the sample holder, fabric specimen, and cover ring were carefully positioned in the dish, and the assembly was sealed using adhesive tape. After that, each test assembly was placed on a turntable and rotated at a speed of 2 r/min for 24 hours. The initial and final weight of the test assembly was recorded to calculate the WVTR in g/m^2/24h, as determined by Equation 1. Three distinct specimens from each fabric type were subjected to testing.

$$WVTR = \frac{m_0 - m_1}{A} \quad (1)$$

$$A = (\frac{\pi d^2}{4}) \times 10^{-6}$$

Where m_0 and m_1 are the weight of the dish, including the water and fabric sample, measured initially and after a 24-hour testing period (g); A is the test area (m^2); d is the inner diameter of the test dish (83 mm).

2.3.4 Thermal properties

The thermal properties of manufactured fabrics, including thermal conductivity, thermal resistance, and heat retention property, were systematically evaluated using the KES-F7 Thermo Labo II Instrument with diverse accessories. Thermal conductivity (W/m·K) and thermal resistance (m^2·K/W) were determined by placing the test specimen between a hot and a cold plate, each having an area of 25 cm^2 and a temperature difference of 10°C. Computation of values for these two properties was accomplished by monitoring the heat transfer from the hot plate through the sample to the cold plate. For the evaluation of heat retention property, the samples were situated on a hot plate with an area of 100 cm^2 and maintained at a temperature 10°C above room temperature. Subsequently, a constant wind velocity of 30 cm/s was applied to the sample surface. The quantification of heat loss through the sample during this process facilitated the calculation of the heat retention rate (%). These thermal evaluations were executed using a sample size of 20 cm × 20 cm, with five repetitions conducted for each sample.

2.3.5 Compressive property

Three compressive characteristics, including compressional linearity (LC), compressional energy (WC), and compressional recoverability (RC), of the sample fabrics were carried out using the KES-FB3-A compression tester. The testing method was based on the instruction manual provided by Kato Tech Co., Ltd. During the evaluation, the tester, equipped with a circular pressing plate, was vertically pressed onto the fabric at a consistent rate, thereby generating a pressure per unit area versus fabric thickness curve. The fabric sample size for this test was 20 cm × 20 cm, and each sample was tested with three repetitions.

2.3.6 Tensile properties

The fabrics' tensile properties, including tensile strength and elongation at break, were evaluated using three test specimens (50 mm x 150 mm) per the ISO 13934-1:2013

standard,[35] utilizing an Instron 5566 test machine. The gauge length was set to 100 mm, and the tensile speed was maintained at 100 mm/min.

2.3.7 Statistical analysis

2.3.7.1 Two-way analysis of variance

Statistical analyses were initially performed using the Statistical Package for the Social Sciences (SPSS 26.0, SPSS Inc., Chicago, USA). The influence of the linear density of inlaid filaments and the blending ratio of staple yarns on the physical, thermal-physiological, and compressive properties of the quilted fabric was assessed through a two-way analysis of variance (ANOVA). Statistical significance was defined as a P-value not greater than 0.05. Additionally, one-factor polynomial regression analysis was conducted using the Origin 2021 software (Microcal Software Inc, Northampton, USA) to establish the relationship between each property and cotton content of surface yarn for a given linear density of inlaid filament.

2.3.7.2 Multiple regression analysis

This study explored the specific relationship between multiple independent variables, including the linear density of inlaid filaments and the blending ratio of surface yarns with individual comfort. Polynomial regression analysis was selected for its common application in investigating intricate or obscure relationships between dependent and independent variables, with SPSS employed for analysis.[36] Before conducting regression analysis, data preprocessing, typically through normalization, was performed to mitigate differences in the magnitude and scale of various experimental datasets.[37] To achieve this standardization, all data in this study were scaled to 0 to 1 using Equation 2 below.

$$z^* = \frac{z - z_{min}}{z_{max} - z_{min}} \quad (2)$$

Where z represents the original data; z_{min} and z_{max} are the minimum and maximum values of the original data, respectively; z^* is the normalized value.

The normalized data were subsequently utilized for the regression analysis, employing a quadratic polynomial model with two independent variables, as depicted in Equation 3 below.

$$y = \beta_0 + \beta_1 x_1 + \beta_2 x_2 + \beta_3 x_1^2 + \beta_4 x_2^2 + \beta_5 x_1 x_2 \quad (3)$$

Where y is the dependent variable; x_1 and x_2 are the independent variables; β_0, β_1, β_2, β_3, β_4, and β_5 are the coefficients to be determined through regression analysis.

The effectiveness of the regression analysis equation was assessed using the coefficient of determination (R^2), which varies between 0 and 1, with 1 indicating a perfect model fit to the data.[38] R^2 is calculated using Equation 4:

$$R^2 = 1 - \frac{\sum_{i=1}^{n}(y_i - \hat{y}_i)^2}{\sum_{i=1}^{n}(y_i - \bar{y})^2} \quad (4)$$

Where y_i are the observed values; $\hat{y}_i$ are the predicted values from the regression model; $\bar{y}$ is the mean of the observed values; and n is the number of observations.

2.3.7.3 Multi-objective optimization using genetic algorithm

This study further investigated the optimal structural parameters of multilayer fabrics to enhance the overall comfort performance. The process involved using fitted regression equations for each comfort property of the multilayered fabric as multi-objective optimization objective functions $f_i(x)$, with the linear density of inlaid yarns and the blending ratio of surface yarns as decision variables. In multi-objective problems, objectives often conflict, making simultaneous optimization challenging.[39] Genetic algorithms, adaptive heuristic search algorithms based on genetics and natural selection, are particularly suitable for addressing such multi-objective optimization problems.[40] They adapt to such challenges by employing specialized fitness functions and methods to enhance solution diversity.[39]

It is noteworthy that during the fabric design process, comfort performance requirements vary depending on the intended applications. For instance, spring fabrics prioritize air and moisture permeability, whereas autumn and winter fabrics emphasize thermal insulation and compressive properties. To cater to the diverse performance demands of fabrics, this study also employed the weighted sum approaches within the evaluation function approach. This method assigns a weight ω_i to each standardized objective function, thereby converting the multi-objective optimization problem into a

single-objective optimization problem.[39] The specific formula 5 is as follows:

$$F_{\min}(x) = \omega_1 f_1(x) + \omega_2 f_2(x) + \cdots + \omega_i f_i(x) \quad (5)$$

Where $f_1(x)$, $f_2(x)$, …, $f_i(x)$ are the normalized objective functions; and ω_1, ω_2, …, ω_i are the corresponding weights.

The weighting coefficients ω_i should satisfy $0 \leq \omega_i \leq 1\ (i = 1, 2, \ldots, n)$ and $\sum_{i=1}^{n} \omega_i = 1$. These coefficients determine the relative importance of each objective function in the composite objective function, with larger coefficients indicating greater importance. Adjusting the size of the weighting coefficients allows the optimization algorithm to balance multiple objectives, thus obtaining a solution that better meets practical needs. In this study, the solution process is implemented using the MATLAB genetic algorithm Toolbox. Initially, weights ω_i were assigned to each standardized objective function, and a composite objective function was constructed. The combined objective function was subsequently optimized using the MATLAB genetic algorithm Toolbox, where the genetic algorithm continuously enhanced solution quality and explored optimal parameter combinations through operations such as selection, crossover, and mutation.

3. Results and discussion

3.1 Physical properties

Figures 2(a)-(d) present the physical properties of the produced PLA/cotton quilted fabrics, including GSM, thickness, stitch density, and surface porosity, along with the corresponding one-factor polynomial regression results. Table 5 provides the detailed two-way ANOVA analysis of these properties. The findings indicate that PLA fabrics with varying GSM, thicknesses, stitch densities, and surface porosities can be achieved by employing diverse linear densities of inlaid PLA filaments and distinct blending ratios of surface staple yarns. It is observed from Figures 2(a) and (b) that the GSM and thickness of the quilted fabrics increase with coarser inlaid filaments while using the same surface yarn. This phenomenon occurs because inlaid filaments with higher linear densities possess greater mass per unit length and larger diameters, resulting in an increase in both GSM and fabric thickness. Moreover, the increased fabric thickness results in a higher fiber count per unit length of the fabric cross-section, a consequence

of the inlaid filaments in this study being merged from the same finer PLA filaments. The ANOVA results in Table 5 further confirm statistically significant associations between the linear densities of inlaid PLA filaments and fabric GSM and thickness ($p = 0.000$ and 0.000, respectively). Nevertheless, the linear density of the inlaid filaments does not significantly influence the fabric stitch density and surface porosity ($p = 0.366$ and 0.381, respectively), as shown in Figures 2(c) and (d). This lack of influence may be due to the inlaid filaments being exclusively inserted in the middle layer of the quilted fabric and not being utilized to fabricate the surface layers.

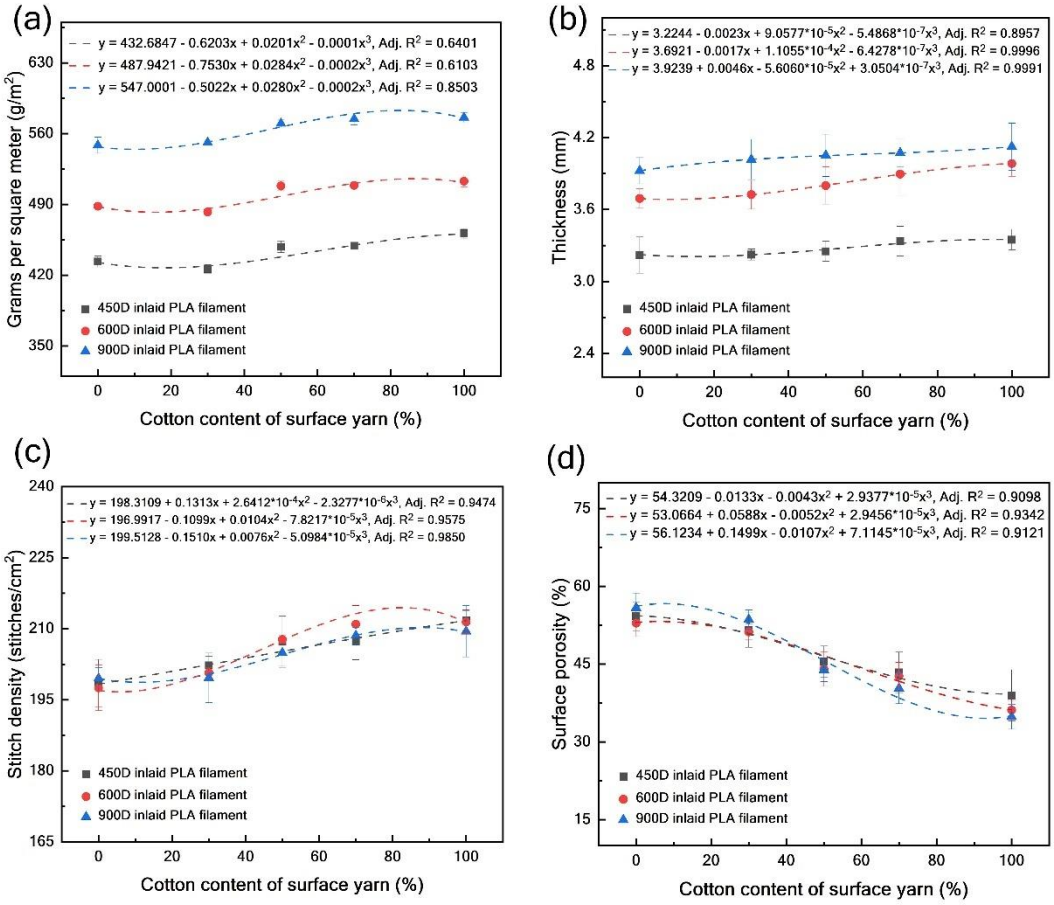

Figure 2. Variations in physical properties of quilted fabrics with varying cotton content of surface yarn for different inlaid PLA filaments: (a) grams per square meter (GSM); (b) thickness; (c) stitch density; (d) surface porosity.

Table 5. Two-way ANOVA results for physical properties of quilted fabrics

Dependent variable	Source	Sum of squares	df	Mean square	F value	P value*
GSM	Inlaid yarn	36307.232	2	18153.616	2096.468	**0.000**

	Blended ratio	2151.831	4	537.958	62.126	**0.000**
Thickness	Inlaid yarn	1.539	2	0.769	494.786	**0.000**
	Blended ratio	0.084	4	0.021	13.444	**0.000**
Stitch density	Inlaid yarn	4.447	2	2.224	1.142	0.366
	Blended ratio	335.844	4	83.961	43.115	**0.000**
Surface porosity	Inlaid yarn	4.922	2	2.461	1.087	0.382
	Blended ratio	636.613	4	159.153	70.27	**0.000**

* P-values in bold indicate significant at ≤ 0.05.

The findings shown in Figures 2(a)-(c) and Table 5 also reveal that there are notable correlations between the blending ratio of surface yarns and the GSM, thickness, stitch density, and the surface porosity of the fabric. Evidently, an increase in the cotton content on the fabric surface corresponds to a rise in fabric GSM, thickness, and stitch density while decreasing surface porosity. This observation could be explained by the variance in hygroscopicity between PLA and cotton. The hygroscopicity of a fiber, defined as its capacity to absorb atmospheric moisture,[41] can be quantified by its moisture regain (MR).[42] Hydrophilic cotton fibers exhibit strong hygroscopicity, with a high MR of approximately 8.5%, whereas hydrophobic PLA fibers demonstrate a weaker ability to absorb atmospheric, with a considerably lower MR of 0.4%-0.6%.[43,44] The calculation equation for the MR of blended yarns is expressed as follows:[45]

$$R_M = p_1R_1 + p_2R_2 + \ldots + p_nR_n = \sum_{i=1}^{n} p_iR_i \quad (6)$$

Where R_i represents the MR of each component; R_M is the MR of the blended yarns; and p_i denotes the mass proportions of the components.

As per Equation (6), it is evident that a higher content of cotton fibers leads to an increased MR in the blended yarn, thereby improving the moisture-absorbing capacity of the yarn. Moreover, the cotton fibers exhibit an increase in cross-sectional area after moisture absorption, known as hygroscopic swelling, while maintaining a nearly constant length.[46] This outcome contributes to greater bending of the yarns within the fabric, ultimately leading to fabric shrinkage, as illustrated in Figure 3. It is noteworthy that this dimensional alteration is irreversible, persisting even after the fabric has undergone the drying process.[47] Consequently, fabrics with a higher cotton content

exhibit higher GSM, thickness, and stitch density. A higher stitch density indicates that the yarns are more tightly arranged per unit area, reducing the gaps within the fabric and thereby resulting in lower surface porosity. Figures 2(a)-(c) also illustrate that while most one-factor polynomial regression models for physical properties exhibit higher adjusted R^2 values over 0.89, the range for GSM is 0.6103-0.8503, indicating moderate model fits. This suggests that one-factor models are insufficient in explaining the variations in GSM well. In the subsequent sections, multiple regression models will be utilized to enhance model accuracy.

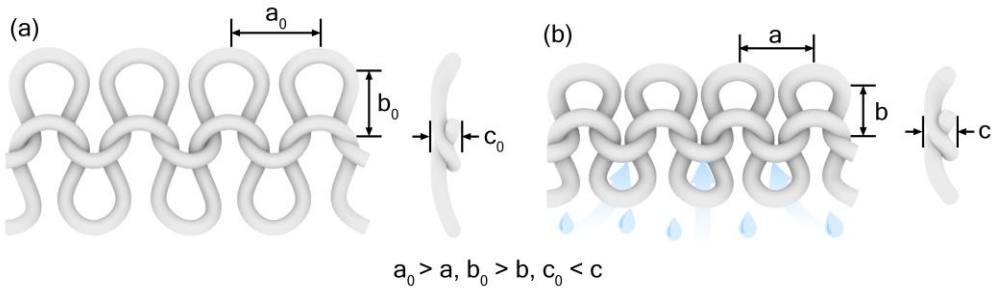

Figure 3. The front and side views of the structure of (a) dry and (b) wet fabrics.

3.2 Air permeability

The air permeability of a fabric reflects its capacity to allow airflow to pass through and can be expressed in terms of air resistance. A lower air resistance indicates that the fabric presents fewer obstacles to airflow, thereby indicating better air permeability. Figure 4 displays the test results of air resistance assessments of quilted fabrics, accompanied by the polynomial regression results. The correlation two-way ANOVA results are presented in Table 6.

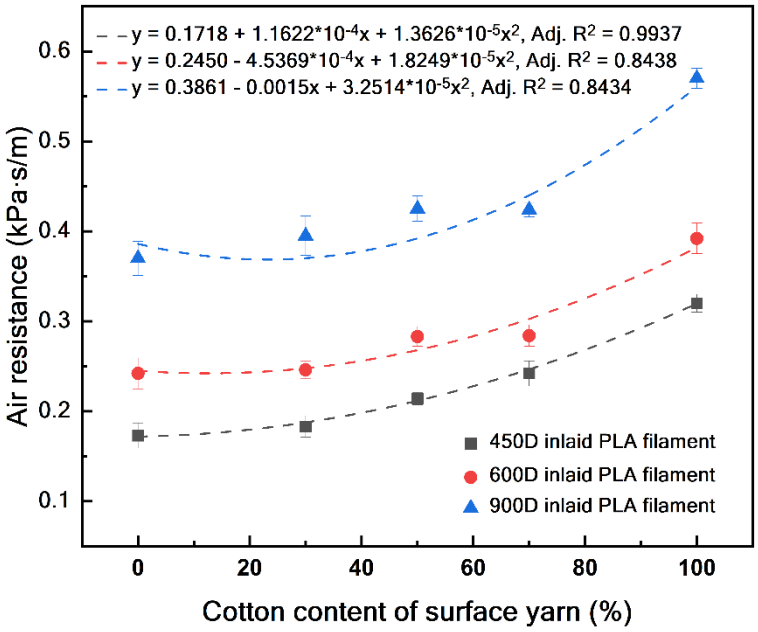

Figure 4. Variations in air resistance of quilted fabrics with varying cotton content of surface yarn for different inlaid PLA filaments.

Table 6. Two-way ANOVA results for air resistance of quilted fabrics

Dependent variable	Source	Sum of squares	df	Mean square	F value	P value*
Air resistance	Inlaid yarn	0.117	2	0.058	307.507	**0.000**
	Blended ratio	0.051	4	0.013	67.719	**0.000**

* P-values in bold indicate significant at ≤ 0.05.

As shown in Figure 4 and Table 6, both the linear density of inlaid PLA filaments and the blending ratio of surface staple yarns have a significant effect on air permeability ($p = 0.000$ and 0.000, respectively). When employing the same staple yarns in the fabric surface, a notable positive relationship is observed between the air resistance of the fabric and the linear density of the inlaid yarns. This phenomenon is attributed to the fact that coarser inlaid yarns result in a thicker and heavier fabric, as illustrated in Figures 2(a) and (b). This results in a lengthier path for air passage through the fabric, leading to decreased airflow, and conversely, higher air resistance. Furthermore, a higher GSM value implies a potentially greater number of fibers per unit area, further contributing to increased air resistance due to increased obstruction to air passage. This observation aligns with the findings reported by Premalatha et al.[48]

On the other hand, when utilizing the same inlaid yarns, it is observed that a higher cotton content on the fabric surface corresponds to greater air resistance. This trend is partially influenced by the inherent properties of the surface yarn. Yarn hairiness is recognized as a significant factor affecting the air permeability of fabrics. Higher hairiness leads to reduced air permeability as the hairiness fills the gaps in the fabric, impeding air circulation.[49] Figure 4 illustrates that fabrics using the 30/70 PLA/cotton blend as surface yarn exhibit relatively lower air resistance compared to those using 50/50 PLA/cotton blend, which can be explained by the lower hairiness value of 3.32 for the 30/70 PLA/cotton blended yarn (Table 2). Additionally, this observation may also be attributed to the higher cotton content prompting yarn expansion and fabric shrinkage, facilitated by enhanced moisture-absorbing capacity, ultimately resulting in a slight rise in fabric stitch density and a decrease in porosity (Figures 2(c) and 2(d)). Evidently, this denser and less porous fabric structure impedes air transmission, thereby contributing to increased air resistance. Furthermore, the rise in cotton content within the fabric is accompanied by an increase in GSM and thickness, collectively impeding airflow between the yarns. The combination of all these factors contributes to the increase in air resistance.

3.3 Water vapor permeability

The capacity of a fabric to transfer perspiration throughout the fabric in the form of water vapor can be assessed in terms of water vapor permeability. In this study, the water vapor permeability of quilted fabrics was evaluated by conducting a 24-hour WVTR test, with results presented in Figure 5 and Table 7.

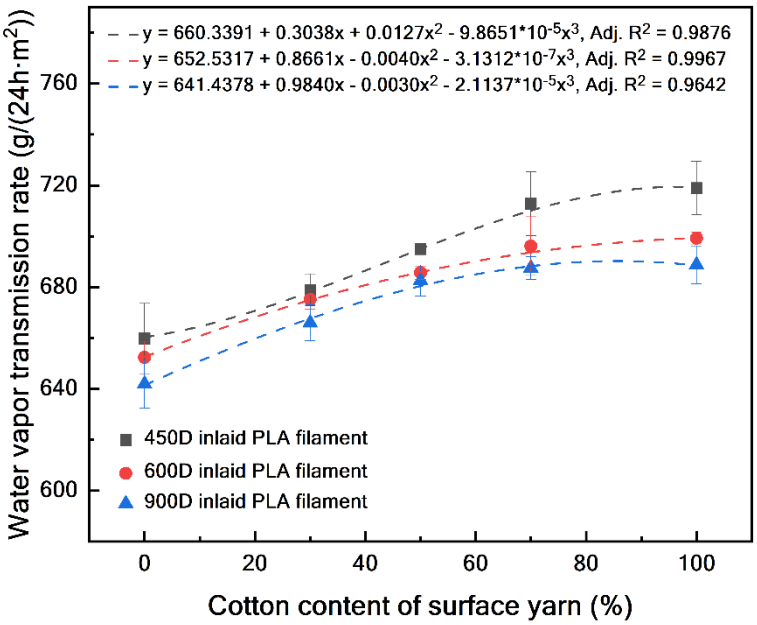

Figure 5. Variations in water vapor transmission rate (WVTR) of quilted fabrics with varying cotton content of surface yarn for different inlaid PLA filaments.

Table 7. Two-way ANOVA results for water vapor transmission rate of quilted fabrics

Dependent variable	Source	Sum of squares	df	Mean square	F value	P value*
WVTR	Inlaid yarn	978.911	2	489.455	25.611	**0.000**
	Blended ratio	5213.560	4	1303.390	68.200	**0.000**

* P-values in bold indicate significant at ≤ 0.05.

The results demonstrate a clear negative association between the WVTR of the fabric and the linear density of the inlaid yarns ($p = 0.000$). This negative association arises from the significant influence of fabric thickness on its water vapor permeability. As noted by Ndlovu et al., thinner fabrics promote more rapid water vapor transfer.[50] Consistent with the airflow transport principle in fabrics, increased fabric thickness results in longer transfer pathways and more fiber contact points, thereby causing greater water vapor transport obstacles. Therefore, the thinner fabrics inserted with 450D PLA filaments exhibit higher WVTR, followed by those with 600D and 900D PLA filaments.

The findings also reveal that the WVTR increases as the cotton proportion in the fabric surface layer increases ($p = 0.000$). This trend is in line with observations made by Das et al. and can be explained by the moisture vapor transmission mechanism.[50,51] The

transmission of vapor through a textile material involves two processes: diffusion and sorption-desorption. Diffusion occurs through the air spaces between the fibers and along the fibers themselves, with the rate depending on the porosity of the material and the water vapor diffusivity of the fiber. Increasing cotton content in fabrics results in higher stitch density and lower surface porosity, limiting water vapor permeability. However, cotton fibers possess high moisture regain rates, leading to blended yarns with greater hygroscopicity as cotton content increases. Moreover, the higher hairiness of cotton fibers provides more moisture absorption sites, further enhancing the fabric's moisture absorption performance. This increased moisture absorption correlates with heightened water vapor diffusion rates and faster sorption-desorption processes within the fabric. Thus, fabrics with greater cotton proportions exhibit accelerated water vapor diffusion and adsorption-desorption processes, ultimately leading to higher WVTR.

3.4 Thermal properties

Figures 6(a)-(c) present the thermal conductivity, thermal resistance, and heat retention of quilted fabrics, respectively, while Table 8 presents the correlation analysis. Thermal conductivity, the inherent ability of a material to conduct heat, is defined as the amount of heat crossing a unit area of the material per unit time per unit temperature gradient.[52] The overall or effective thermal conductivity (k) of fabric can be calculated by Fourier's law of conduction:[53]

$$k = \frac{Q \cdot h}{A \cdot \Delta T_0} \left(\frac{W}{m} \cdot K\right) \tag{7}$$

Where Q is the heat consumption; h represents the thickness of the sample (m); k denotes the thermal conductivity of the sample (W/m·K); A corresponds to the area of the heat plate (m^2); ΔT_0 represents the temperature difference.

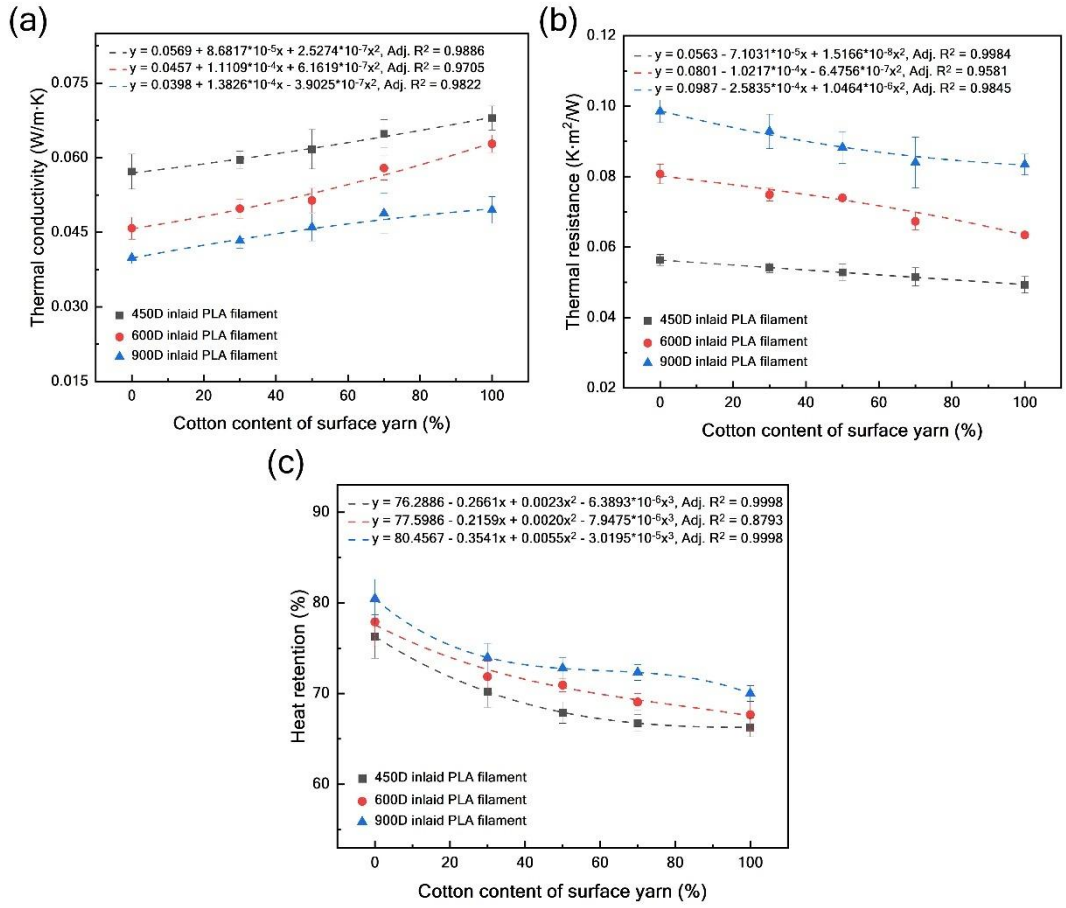

Figure 6. Variations in thermal properties of quilted fabrics with varying cotton content of surface yarn for different inlaid PLA filaments: (a) thermal conductivity; (b) thermal resistance; (c) heat retention.

Table 8. Two-way ANOVA results for thermal properties of quilted fabrics

Dependent variable	Source	Sum of squares	df	Mean square	F value	P value*
Thermal conductivity	Inlaid yarn	0.001	2	0.000	111.886	**0.000**
	Blended ratio	0.000	4	0.000	23.426	**0.000**
Thermal resistance	Inlaid yarn	0.003	2	0.002	270.079	**0.000**
	Blended ratio	0.000	4	0.000	13.059	**0.001**
Heat retention	Inlaid yarn	48.956	2	24.478	106.016	**0.000**
	Blended ratio	189.218	4	47.305	204.877	**0.000**

* P-values in bold indicate significant at ≤ 0.05.

The difference observed in Figure 6(a) between samples produced with the same surface yarns indicates that thermal conductivity values highly depend on the types of

inlaid yarns, supported by the p-value of 0.000 in Table 8. This is because the thermal conductivity of a fabric is strongly influenced by its thickness, while the inlaid yarns influence the thickness.[54] Previous research explained that increased thickness typically leads to a greater volume of trapped air within the fabric structure.[54] While air is a known most insulative material with a thermal conductivity of 0.025 W/(m·K),[55] the increased presence of trapped air within the fabric subsequently results in reduced thermal conductivity.[6]

Figure 6(a) also illustrates a slight increase in thermal conductivity as the surface cotton proportion increases (p = 0.000). This phenomenon might be because fabrics with a greater cotton proportion possess a higher GSM and stitch density, along with lower surface porosity, resulting in increased fibrous material and decreased trapped air per unit area. This increase in fibrous materials, having a higher thermal conductivity than air, increases their contact points with each other and influences the flow of heat between fabrics.[56]

Thermal resistance is another crucial indicator for evaluating the thermal-physiological comfort of fabrics, and refers to the ability of the material that prevents the heat flowing through the fabric.[21] It is defined as the ratio of temperature difference to the rate of heat flow per unit area.[53]

$$R = \frac{\Delta T_0}{\frac{Q}{A}} \left(m^2 \cdot \frac{K}{W} \right) \tag{8}$$

Where Q is the heat consumption; A corresponds to the area of the heat plate (m^2); ΔT_0 represents the temperature difference.

Thermal resistance can also be calculated by the effective thermal conductivity of fabric:

$$R = \frac{h}{k} \ (m^2 \cdot K/W) \tag{9}$$

Where h is fabric thickness (m); and k is thermal conductivity (W/m·K).

Equation (9) clearly illustrates the reciprocal relationship between fabric thermal

resistance and thermal conductivity, which is further supported by the thermal resistance test results depicted in Figure 6(b). Contrary to the thermal conductivity results, the fabric's thermal resistance shows a positive relationship with the linear density of the inlaid filaments and a negative relationship with the content of cotton fibers on the fabric surface (p = 0.000 and 0.001, respectively). The higher the thermal resistance, the better the thermal insulation of the fabric. The thermal resistance results indicate that selecting 900D PLA filament yarns as the inlaid filaments, with 100% PLA staple yarn as surface yarn, contributes to increased thermal resistance in the fabric, thereby enhancing heat retention. This conclusion also perfectly agrees with the test results of heat retention in Figure 6(c) (p = 0.000 and 0.000, respectively).

3.5 Compressive property

The compressive test under low load simulates human hand compression on the fabric, and the resulting data are valuable for assessing the fabric's tactile property. The test results for the compressive characteristics (LC, WC, and RC) of quilted fabrics are shown in Figures 7(a)-(c), with the statistical analysis detailed in Table 9.

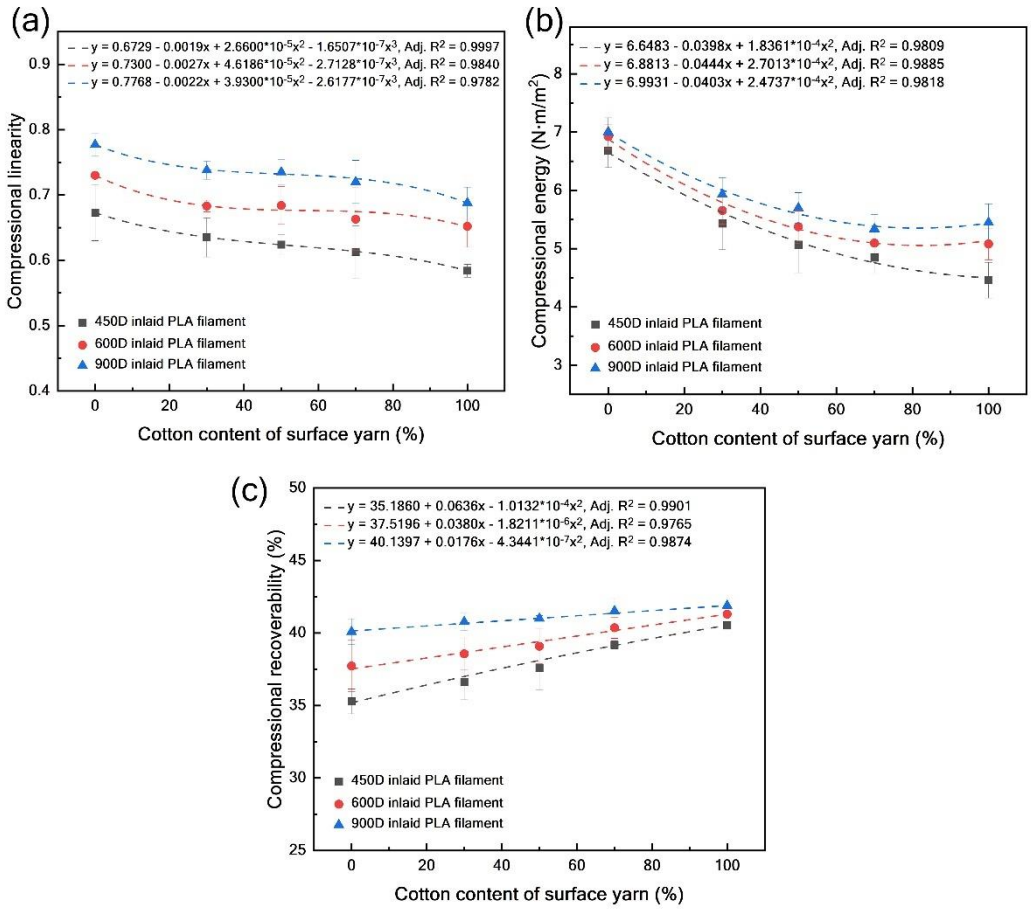

Figure 7. Variations in compressive properties of quilted fabrics with varying cotton content of surface yarn for different inlaid PLA filaments: (a) compressional linearity (LC); (b) compressional energy (WC); (c) compression recoverability (RC).

Table 9. Two-way ANOVA results for compressive properties of quilted fabrics

Dependent variable	Source	Sum of squares	df	Mean square	F value	P value*
LC	Inlaid yarn	0.028	2	0.014	581.128	**0.000**
	Blended ratio	0.012	4	0.003	121.827	**0.000**
WC	Inlaid yarn	0.863	2	0.431	25.078	**0.000**
	Blended ratio	6.855	4	1.714	99.634	**0.000**
RC	Inlaid yarn	25.779	2	12.890	26.829	**0.000**
	Blended ratio	23.289	4	5.822	12.119	**0.002**

* P-values in bold indicate significant at ≤ 0.05.

Figures 7(a)-(c) and the ANOVA results in Table 9 show that LC, WC, and RC increase with the rising linear density of inlaid yarns (p = 0.000, 0.000, and 0.000, respectively). LC, a dimensionless parameter, reflects the linearity of the compression-thickness curve, where higher LC values indicate firmer compression. WC represents the energy required for the compressive deformation of a textile material, with higher WC values indicating greater compressive susceptibility. Fabric thickness has been established as a crucial factor influencing LC and WC values, as thicker fabrics tend to be more compressible due to the increased volume of material that can be deformed under pressure.[57,58] Consequently, the quilted fabric inlaid with coarser PLA filaments exhibits increased thickness, subsequently leading to enhanced compressibility. Additionally, the RC parameter characterizes the fabric's ability to rapidly recover after compressive deformation, with higher RC values indicating superior recoverability.[59] The results also highlight that coarser inlaid PLA filaments are associated with improved fabric recoverability, possibly attributed to the higher elasticity of coarser inlaid filaments.

The blending ratio of surface yarns also exerts a significant influence on fabric compression. Specifically, as the proportion of cotton in the fabric surface increases, LC and WC decrease while RC increases (p = 0.000, 0.000, and 0.002, respectively). This behavior might be attributed to the observation that compressive values of the

knitted fabrics decrease with increasing stitch density and decreasing surface porosity, which can be explained by the fabric structure.[57] Fabrics with a higher surface cotton proportion exhibit a greater stitch density and lower surface porosity, thereby enhancing compressive resistance and minimizing the presence of compressible air gaps, ultimately decreasing compressibility. Conversely, the results also reveal that an increased content of cotton fibers on the surface enhances the elastic recovery of the fabric after compression, implying these fabrics possess a greater capacity to overcome the recovery resistance.

3.6 Determination of optimal fabric parameters based on regression analysis and genetic algorithm

To characterize the relationship between fabric structural parameters and fabric comfort properties, all experimental data were initially normalized using SPSS. Subsequently, eight polynomial regression equations for fabric comfort properties were established based on the quadratic polynomial model described in Equation 3. The independent variables include the linear density of the inlaid yarns (x_1) and the blending ratio of the surface yarns (x_2), while the dependent variables comprised air permeability ($f_1(x)$), water vapor permeability ($f_2(x)$), thermal conductivity ($f_3(x)$), thermal resistance ($f_4(x)$), heat retention ($f_5(x)$), LC ($f_6(x)$), WC ($f_7(x)$), and RC ($f_8(x)$). The regression models for each comfort property, along with their corresponding R^2 values, are detailed in Table 10. The high R^2 values, ranging from 0.973 to 0.991, indicate the statistical validity of these models.

Table 10. Regression models and R^2 values for fabric comfort properties

Properties	Equations	R^2
Air permeability	$f_1(x) = 0.023 + 0.398x_1 - 0.137x_2 + 0.084x_1^2 + 0.489x_2^2 + 0.097x_1x_2$	0.985
Water vapor permeability	$f_2(x) = 0.209 - 0.452x_1 + 1.326x_2 + 0.278x_1^2 - 0.569x_2^2 - 0.165x_1x_2$	0.978
Thermal conductivity	$f_3(x) = 0.554 - 1.056x_1 + 0.456x_2 + 0.501x_1^2 + 0.039x_2^2 - 0.082x_1x_2$	0.973
Thermal resistance	$f_4(x) = 0.185 + 1.463x_1 - 0.278x_2 - 0.643x_1^2 + 0.071x_2^2 - 0.152x_1x_2$	0.990

Heat retention	$f_5(x) = 0.676 + 0.47x_1 - 1.46x_2 - 0.167x_1^2 + 0.766x_2^2 + 0.018x_1x_2$	0.980
LC	$f_6(x) = 0.442 + 1.048x_1 - 0.557x_2 - 0.497x_1^2 + 0.143x_2^2 - 0.004x_1x_2$	0.986
WC	$f_7(x) = 0.861 + 0.36x_1 - 1.76x_2 - 0.236x_1^2 + 0.952x_2^2 + 0.213x_1x_2$	0.987
RC	$f_8(x) = 0.003 + 1.083x_1 + 0.729x_2 - 0.335x_1^2 + 0.055x_2^2 - 0.526x_1x_2$	0.991

This study further employs multi-objective optimization to determine fabric parameters for optimal overall fabric comfort. In such optimization, some objectives require maximization while others necessitate minimization. For instance, minimizing air resistance improves air permeability, while maximizing moisture permeability enhances its effectiveness. To address this, the duality principle in optimization suggests transforming maximization problems into minimization ones by multiplying the objective function by -1.[60] This principle simplifies the handling of mixed objectives, as many optimization algorithms are designed for single-type problems, typically minimization. Considering this principle and the specific comfort attributes in this study, the following weighted objective function was constructed based on Equation 10:

$$F(x)_{min} = \omega_1 f_1(x) - \omega_2 f_2(x) + \omega_3 f_3(x) - \omega_4 f_4(x) - \omega_5 f_5(x) + \omega_6 f_6(x) - \omega_7 f_7(x) - \omega_8 f_8(x) \quad (10)$$

Where $f_1(x)$ is the normalized function for air permeability; $f_2(x)$ for water vapor permeability; $f_3(x)$ for thermal conductivity; $f_4(x)$ or thermal resistance; $f_5(x)$ for heat retention; $f_6(x)$ for LC; $f_7(x)$ for WC; $f_8(x)$ for RC, and ω_1, ω_2, …, ω_8, are the corresponding weight coefficients for each normalization function. The negative symbol indicates the conversion of an objective function from maximization to minimization type.

Various weight combinations have been devised to cater to the diverse requirements of different fabric applications. Specifically, distinct weight combinations were formulated to achieve a harmonious balance of various comfort attributes, enhancing air and moisture permeability and improving thermal and compressive properties, respectively. These weight combinations are detailed in Table 11.

Table 11. Weight combinations for fabric comfort properties optimization

Case	Objective	ω_1	ω_2	ω_3	ω_4	ω_5	ω_6	ω_7	ω_8
1	Balance of various comfort properties	0.251	0.251	0.083	0.083	0.083	0.083	0.083	0.083
2	Air and moisture permeability	0.29	0.29	0.07	0.07	0.07	0.07	0.07	0.07
3	Thermal and compressive properties	0.2	0.2	0.1	0.1	0.1	0.1	0.1	0.1

Based on the assigned weighting coefficients, the MATLAB genetic algorithm toolbox was employed to solve the model. The operating parameters of the genetic algorithm are as follows: population size of 100, population type as double vector, maximum number of generations set to 100, number of problem variables set to 2, scaling function using the ranking method, selection function as stochastic uniform, crossover fraction of 0.8, crossover function as crossoverscattered, migration fraction of 0.2, and mutation function as mutationgaussian. Table 12 presents the optimal parameter combinations for three sets of weighting coefficients. The findings indicate that in Case 1, selecting 450D PLA for the inlaid yarn and a 50/50 PLA/cotton blend for the surface yarn (Fabric 3) achieves overall optimal comfort properties. The results from Case 2 are consistent with Case 1, showing that Fabric 3 exhibits enhanced air and moisture permeability. In Case 3, using 900D PLA for the inlaid yarn and 100% PLA for the surface yarn (Fabric 11) improves thermal and compressive properties.

Table 12. Optimized fabric parameters

Case	Optimization objectives	Inlaid yarn	Surface yarn	Fabric no.
1	Balance of various comfort properties	450D PLA filament	50/50 PLA/cotton blended yarn	3
2	Air and moisture permeability	450D PLA filament	50/50 PLA/cotton blended yarn	3
3	Thermal and compressive properties	900D PLA filament	100% PLA yarn	11

Table 13 illustrates the comfort performance of two optimized fabrics, Fabric 3 and Fabric 11, alongside fabrics with similar GSM and thickness from three earlier studies for comparison.[17,59,61] Fabric 3 in this study shows lower air resistance (0.214 kPa·s/m)

than that reported in previous study 1 (0.269 kPa·s/m), indicating superior air permeability. Additionally, Fabric 3 exhibits a significantly higher WVTR of 694.931 g/m²/24h compared to the fabric from previous Study 2 (289.310 g/m²/24h), highlighting excellent moisture management. Regarding thermal properties, Fabric 3 demonstrates thermal conductivity similar to the fabric in previous study 3, while its heat retention (67.907%) exceeds that of the fabric in an earlier study 2 (21.380%). Fabric 3 also exhibits superior compressibility, with a WC of 5.068 N·m/m², higher than that in previous study 1. Therefore, the multilayer fabrics developed in the present study demonstrate improved overall comfort properties compared to earlier fabrics with similar specifications.

Table 13. Comparison of comfort performance of optimized fabrics and previous studies

Properties	Fabric 3	Fabric 11	Previous study 1[59]	Previous study 2[61]	Previous study 3[17]
Mass (g/m^2)	448.073	548.594	454.000	433.000	443.000
Thickness (mm)	3.252	3.924	3.363	3.370	2.620
Air resistance (kPa·s/m)	0.214	0.370	0.269	--	--
WVTR (g/m^2/24h)	694.931	641.949	--	289.310	--
Thermal conductivity (W/m·K)	0.062	0.040	--	--	0.061
Thermal resistance (m^2·K/W)	0.053	0.099	--	--	--
Heat retention (%)	67.907	80.465	--	21.380	--
LC	0.624	0.777	0.258	--	--
WC (N·m/m^2)	5.068	7.003	2.002	--	--
RC (%)	37.603	40.087	38.875	--	--

Note: Superscripts 59, 61, and 17 denote cited reference numbers.

3.7 Durability

In addition to comfort, dimensional change and tensile properties are crucial indicators for evaluating the usability of fabrics, particularly in terms of performance stability after multiple washings. To assess the durability of the produced fabrics, optimized Fabric 3 and Fabric 11 were selected and subjected to 20 repetitive washing cycles following the ISO 6330:2021 standard. The dimensional change, tensile strength, and elongation at break of these fabrics were measured after the 1st, 5th, 15th, and 20th

wash cycles. All test results are summarized in Table 14.

Table 14. Dimensional change and tensile properties of optimized fabrics after multiple washing cycles

Properties		Fabric 3				Fabric 11			
		Washed 1 time	Washed 5 times	Washed 15 times	Washed 20 times	Washed 1 time	Washed 5 times	Washed 15 times	Washed 20 times
Dimensional change (%)	Warp direction	-10.67 (± 0.47)	-12.47 (± 0.41)	-11.33 (± 0.94)	-13.33 (± 0.47)	-4.67 (± 0.47)	-5.33 (± 0.94)	-5.80 (± 0.86)	-5.67 (± 0.94)
	Weft direction	-12.50 (± 0.41)	-15.00 (± 0.82)	-16.50 (± 0.71)	-16.17 (± 0.62)	-9.50 (± 0.41)	-10.33 (± 0.47)	-9.83 (± 0.24)	-10.50 (± 0.41)
Tensile strength (N)	Warp direction	231.56 (± 18.46)	227.69 (± 14.67)	217.66 (± 23.54)	215.30 (± 25.46)	330.55 (± 19.87)	325.80 (± 18.18)	326.60 (± 26.13)	325.48 (± 8.98)
	Weft direction	379.12 (± 25.84)	369.01 (± 28.93)	370.62 (± 23.78)	372.82 (± 10.18)	506.98 (± 29.79)	498.83 (± 31.56)	503.75 (± 21.24)	496.59 (± 23.94)
Elongation at break (%)	Warp direction	107.06 (± 4.87)	100.65 (± 4.93)	105.17 (± 4.39)	94.75 (± 7.31)	98.00 (± 9.90)	91.94 (± 3.58)	82.39 (± 4.32)	91.28 (± 4.76)
	Weft direction	152.92 (± 10.87)	156.17 (± 7.59)	158.61 (± 13.68)	154.75 (± 6.48)	66.28 (± 5.34)	73.61 (± 6.84)	64.18 (± 1.34)	66.95 (± 5.84)

Note: The values enclosed within parentheses correspond to the standard deviations.

The results in Table 14 indicate that dimensional changes in the fabrics primarily occur during the initial washing cycle, consistent with previous findings.[62] Subsequent washing cycles show stabilized dimensional changes, all within 3.67%, indicating good dimensional stability. Shrinkage and distortion of the fabrics post-washing are predominantly influenced by fabric structural parameters such as yarn density and knitting pattern, as well as the mechanical processes of washing, drying agitation, and the release of strain accumulated during manufacturing. Furthermore, as observed in Table 14, Fabric 3 exhibits higher dimensional changes in both warp and weft directions compared to Fabric 11. This difference may stem from the higher cotton content on the surface of Fabric 3, which enhances hygroscopicity and swells upon moisture absorption, thereby increasing fabric shrinkage.

On the other hand, the tensile strength of both fabrics in the warp and weft directions

shows no significant decrease after several washes, consistently exceeding 215.30 N, demonstrating stable strength suitable for daily use. Table 14 also illustrates that Fabric 11 exhibits higher tensile strength and lower elongation compared to fabric 3. This phenomenon arises because Fabric 3 incorporates 450D PLA inlaid filaments, whereas Fabric 11 utilizes 900D PLA inlaid filaments. Inserting 900D PLA filaments allows Fabric 11 to withstand greater tensile forces and reduces fiber slippage during stretching. Notably, both fabrics display higher tensile strength in the weft direction due to the insertion of inlaid yarns along the weft during manufacturing. Additionally, both fabrics exhibit elongation exceeding 64.18%, a characteristic determined by the loop structure of the knitted fabrics. The elongation of the fabrics remains consistent after multiple washings, further emphasizing their excellent stability.

4. Conclusions

Comfort is widely acknowledged as a vital fabric property, and its assessment relies on critical indicators, including air permeability, water vapor permeability, thermal and compressive properties. PLA and PLA/cotton blended yarns hold particular significance in the exploitation of natural textile products. This study developed diverse multilayered quilted fabrics by employing different PLA filaments and PLA/cotton blended yarns as inlaid and surface yarns, respectively. A comprehensive investigation was conducted to systematically assess the impact of the linear density of inlaid yarns and the blending ratios of surface yarns on the comfort properties of the fabrics. Statistical analysis indicates that the two independent variables are significant for the air permeability, water vapor permeability, thermal and compressive properties of the quilted fabrics. Specifically, fabrics inlaid with coarser filaments typically display higher GSM and thickness, adversely affecting air and water vapor permeability while enhancing thermal insulation and compressive properties. Additionally, fabrics with a higher proportion of surface cotton show increased GSM, thickness, stitch density, and reduced surface porosity, leading to lower air permeability, thermal retention, and compressibility, but improved water vapor permeability owing to heightened hydrophilicity.

Multiple regression models were developed, all with R^2 values exceeding 0.97, to quantify the relationships between yarn parameters and comfort properties. To determine the optimal yarn parameters, a multi-objective optimization model was formulated and solved using the MATLAB genetic algorithm toolbox. The results show

that selecting 450D PLA for the inlaid yarn and a 50/50 PLA/cotton blend for the surface yarn achieves outstanding overall comfort properties, and enhanced air and moisture permeability. For enhanced thermal and compressive properties, using 900D PLA for the inlaid yarn and 100% PLA for the surface yarn is suggested. Subsequent durability tests on the optimized fabrics reveal that dimensional changes stabilize within 3.67% after the initial wash, with minimal changes observed in tensile properties, demonstrating stable fabric performance even after repeated washing. The findings are expected to offer valuable insights for designing multilayered quilted fabrics by utilizing PLA filaments and PLA/cotton blended yarns. These eco-friendly fabrics, developed with enhanced comfort properties in this study, are versatile in applications, including winter apparel, military gear, skiwear, bedding, furniture upholstery, industrial insulation, and medical garments.

Declarations

The authors declare no potential conflicts of interest.

Funding

This work was supported by the Hong Kong Research Institute of Textiles and Apparel Limited and the Innovation and Technology Commission of The Government of the Hong Kong Special Administrative Region of China in the form of an ITF project (Ref. No. ITP/030/21TP).

References

1. Fattahi FS, Khoddami A and Avinc O. Sustainable, Renewable, and Biodegradable Poly(Lactic Acid) Fibers and Their Latest Developments in the Last Decade. In: Muthu SS and Gardetti MA (eds) *Sustainability in the Textile and Apparel Industries: Sourcing Synthetic and Novel Alternative Raw Materials*. Cham: Springer International Publishing, 2020, pp.173-194.
2. Błędzki A, Jaszkiewicz A, Urbaniak M, et al. Biocomposites in the Past and in the Future. *Fibres Text East Eur* 2012; 20. DOI: 10.1016/0375-9474(88)90301-6.
3. Guruprasad R, Vivekanandan M, Arputharaj A, et al. Development of cotton-rich/polylactic acid fiber blend knitted fabrics for sports textiles. *J Ind Text* 2015; 45: 405-415. DOI: 10.1177/1528083714555779.
4. Yang Y, Zhang M, Ju Z, et al. Poly(lactic acid) fibers, yarns and fabrics: Manufacturing, properties and applications. *Text Res J* 2021; 91: 1641-1669. DOI: 10.1177/0040517520984101.

5. Nampoothiri KM, Nair NR and John RP. An overview of the recent developments in polylactide (PLA) research. *Bioresour Technol* 2010; 101: 8493-8501. DOI: 10.1016/j.biortech.2010.05.092.
6. Jabbar A, Tausif M, Tahir HR, et al. Polylactic acid/lyocell fibre as an eco-friendly alternative to polyethylene terephthalate/cotton fibre blended yarns and knitted fabrics. *J Text Inst* 2020; 111: 129-138. DOI: 10.1080/00405000.2019.1624070.
7. Kannan TG, Wu CM and Cheng KB. Effect of different knitted structure on the mechanical properties and damage behavior of Flax/PLA (Poly Lactic acid) double covered uncommingled yarn composites. *Composites Part B* 2012; 43: 2836-2842. DOI: 10.1016/j.compositesb.2012.04.047.
8. Yang QB. The elasticity of PLA fiber blended yarn. *Adv Mater Res* 2012; 496: 463-466. DOI: 10.4028/www.scientific.net/AMR.496.463.
9. Manich AM, Miguel R, Silva MJdS, et al. Effect of processing and wearing on viscoelastic modeling of polylactide/wool and polyester/wool woven fabrics subjected to bursting. *Text Res J* 2014; 84: 1961-1975. DOI: 10.1177/0040517514530034.
10. Chattopadhyay S and Guruprasad R. Blending of cotton and poly (lactic acid) fiber: Combined optimization of blend ratio and yarn twist using mixture-process design. *J Nat Fibers* 2021; 18: 631-643. DOI: 10.1080/15440478.2019.1642825.
11. Jantip S, Porntip SB and Suwanruji P. Effect of pretreatment and dyeing processes on the physical properties of Poly (Lactic acid)/Cotton blended fabric. *Adv Mater Res* 2012; 486: 253-259. DOI: 10.4028/www.scientific.net/AMR.486.253.
12. Phatthalung IN, Sae-be P, Suesat J, et al. Investigation of the optimum pretreatment conditions for the knitted fabric derived from PLA/cotton blend. *Int J Biosci, Biochem Bioinf* 2012; 2: 179. DOI: 10.7763/IJBBB.2012.V2.96.
13. Huang H, Ma W, Zhang S, et al. Optimal dyeing systems for resistance to the physical strength loss of the PLA/cotton blended fabric. *J Appl Polym Sci* 2011; 120: 886-895. DOI: 10.1002/app.33190.
14. Abbasi SA, Marmaralı A and Ertekin G. Thermal comfort properties of weft knitted quilted fabrics. *Int J Cloth Sci Technol* 2020; 32: 837-847. DOI: 10.1108/IJCST-07-2019-0111.
15. Spencer DJ. *Knitting technology: a comprehensive handbook and practical guide*. 3rd ed. Cambridge England: Woodhead publishing limited, 2001.
16. Prakash C and Ramakrishnan G. Effect of blend proportion on thermal behaviour of bamboo knitted fabrics. *J Text Inst* 2013; 104: 907-913. DOI: 10.1080/00405000.2013.765090.
17. Arumugam V, Mishra R, Militky J, et al. Investigation on thermo-physiological and compression characteristics of weft-knitted 3D spacer fabrics. *J Text Inst* 2017; 108: 1095-1105. DOI: 10.1080/00405000.2016.1220035.
18. Gokarneshan N. Comfort properties of textiles: a review of some breakthroughs in recent research. *JOJ Mater Sci* 2019; 5: 1-5. DOI: 10.19080/JOJMS.2019.05.555662.
19. Cui P, Wang F, Wei A, et al. The performance of kapok/down blended wadding. *Text Res J* 2010; 80: 516-523. DOI: 10.1177/0040517508097522.
20. El-Ola SMA, Elshakankery MH and Kotb RM. Integration of nanocomposite finishing on polyester fabric for enhanced UV protection, performance, and comfort

properties. *J Eng Fibers Fabr* 2022; 17: 1-17. DOI: 10.1177/15589250221119447.
21. Onal L and Yildirim M. Comfort properties of functional three-dimensional knitted spacer fabrics for home-textile applications. *Text Res J* 2012; 82: 1751-1764. DOI: 10.1177/0040517512444331.
22. Yu A, Sukigara S and Takeuchi S. Effect of inlaid elastic yarns and inlay pattern on physical properties and compression behaviour of weft-knitted spacer fabric. *J Ind Text* 2022; 51: 2688S-2708S. DOI: 10.1177/1528083720947740.
23. ASTM D1907-01. Standard Test Method for Linear Density of Yarn (Yarn Number) by the Skein Method.
24. ASTM D2256. Standard Test Method for Tensile Properties of Yarns by the Single-Strand Method.
25. ASTM D5647-07. Standard Guide for Measuring Hairiness of Yarns by the Photo-Electric Apparatus.
26. ASTM D1425/D1425M-14. Standard Test Method for Evenness of Textile Strands Using Capacitance Testing Equipment.
27. ASTM D1422/D1422M-13. Standard Test Method for Twist in Single Spun Yarns by the Untwist-Retwist Method.
28. Oner E, Topcuoglu S and Kutlu O. The effect of cotton fibre characteristic on yarn properties. In: *IOP Conference Series: Materials Science and Engineering* 2018, p.012057. IOP Publishing.
29. ISO 6330:2021. Textiles — Domestic washing and drying procedures for textile testing.
30. ISO 139:2005. Textiles — Standard atmospheres for conditioning and testing.
31. ASTM D3776-09. Standard Test Methods for Mass Per Unit Area (Weight) of Fabric.
32. ASTM D1777-96. Standard Test Method for Thickness of Textile Materials.
33. ASTM D3887-96. Standard Specification for Tolerances for Knitted Fabrics.
34. BS 7209:1990. Specification for water vapour permeable apparel fabrics.
35. ISO 13934-1:2013. Textiles — Tensile properties of fabrics.
36. DeCoster J and Claypool H. Data analysis in SPSS. 2004.
37. Chen S-H and Kuo C-FJ. Functional dyeable polypropylene fabric development and process parameter optimization. Part II: Development of graphene thermal insulation dyeable polypropylene fabric with process parameter optimization. *Text Res J* 2023; 93: 3717-3735. DOI: 10.1177/00405175221147720.
38. Chicco D, Warrens MJ and Jurman G. The coefficient of determination R-squared is more informative than SMAPE, MAE, MAPE, MSE and RMSE in regression analysis evaluation. *Peerj computer science* 2021; 7: 1-24. DOI: 10.7717/peerj-cs.623.
39. Konak A, Coit DW and Smith AE. Multi-objective optimization using genetic algorithms: A tutorial. *Reliab Eng Syst Saf* 2006; 91: 992-1007. DOI: 10.1016/j.ress.2005.11.018.
40. Padhi P, Mahapatra S, Yadav S, et al. Multi-objective optimization of wire electrical discharge machining (WEDM) process parameters using weighted sum genetic algorithm approach. *J Adv Manuf Syst* 2016; 15: 85-100. DOI: 10.1142/S0219686716500086.

41. Li Y and Luo Z. Physical mechanisms of moisture diffusion into hygroscopic fabrics during humidity transients. *J Text Inst* 2000; 91: 302-316. DOI: 10.1080/00405000008659508.
42. Murthy HVS. *Introduction to textile fibres*. India: WPI India, 2016.
43. Farrington D, Lunt J, Davies S, et al. Poly (lactic acid) fibers. In: Blackburn R (ed) *Biodegradable and sustainable fibres*. Netherlands: Elsevier, 2005, pp.191-220.
44. Wang X, Li W, Xu W, et al. Study on the surface temperature of fabric in the process of dynamic moisture liberation. *Fibers Polym* 2014; 15: 2437-2440. DOI: 10.1007/s12221-014-2437-4.
45. Zeidman M. The Correct Calculation of the Moisture Regain of Fiber Mixtures. *Text Res J* 1980; 50: 393-394. DOI: 10.1177/004051758005000614.
46. Preston J and Nimkar M. Measuring the swelling of fibres in water. *J Text Inst* 1949; 40: P674-P688. DOI: 10.1080/19447014908664692.
47. Saville BP. *Physical testing of textiles*. Netherlands: Elsevier, 1999.
48. Premalatha C, Kumar MR, Udaya Krithika S, et al. Analysis of thermal comfort properties of tri-layer knitted fabrics. *J Nat Fibers* 2023; 20: 2164107. DOI: 10.1080/15440478.2022.2164107.
49. Ivanovska A, Reljic M, Kostic M, et al. Air permeability and water vapor resistance of differently finished cotton and cotton/elastane single jersey knitted fabrics. *J Nat Fibers* 2022; 19: 5465-5477. DOI: 10.1080/15440478.2021.1875383.
50. Ndlovu LN, Siddiqui Q, Omollo E, et al. Physical properties of plain single jersey-knitted fabrics made from blended and core-spun polysulfonamide/cotton yarns. *Text Res J* 2015; 85: 262-271. DOI: 10.1177/0040517514542145.
51. Das B, Das A, Kothari V, et al. Moisture flow through blended fabrics–Effect of hydrophilicity. *J Eng Fibers Fabr* 2009; 4: 20-28. DOI: 10.1108/09556220910995738.
52. El Wazna M, El Fatihi M, El Bouari A, et al. Thermo physical characterization of sustainable insulation materials made from textile waste. *J Build Eng* 2017; 12: 196-201. DOI: 10.1016/j.jobe.2017.06.008.
53. Siddiqui MOR and Sun D. Development of experimental setup for measuring the thermal conductivity of textiles. *Clothing Text Res J* 2018; 36: 215-230. DOI: 10.1177/0887302x18768041.
54. Terliksiz S, Kalaoğlu F and Eryürük SH. Analysis of thermal comfort properties of jacquard knitted mattress ticking fabrics. *Int J Cloth Sci Technol* 2016; 28: 105-114. DOI: 10.1108/ijcst-02-2015-0028.
55. Elmogahzy Y. *Engineering textiles: Integrating the design and manufacture of textile products*. Netherlands: Elsevier, 2019.
56. Afzal A, Ahmad S, Rasheed A, et al. Influence of fabric parameters on thermal comfort performance of double layer knitted interlock fabrics. *Autex Res J* 2017; 17: 20-26. DOI: 10.1515/aut-2015-0037.
57. Stojanović S, Geršak J and Trajković D. Compression properties of knitted fabrics printed by sublimation transfer printing technique. *Adv Technol* 2021; 10: 46-53. DOI: 10.5937/savteh2101046s.
58. Nayak R, Punj S, Chatterjee K, et al. Comfort properties of suiting fabrics. *Indian J Fibre Text Res* 2009; 34: 122-128.

59. Liu Y and Hu H. Compression property and air permeability of weft-knitted spacer fabrics. *J Text Inst* 2011; 102: 366-372. DOI: 10.1080/00405001003771200.
60. Deb K. Multi-objective optimisation using evolutionary algorithms: an introduction. *Multi-objective evolutionary optimisation for product design and manufacturing*. Springer, 2011, pp.3-34.
61. Chen Q, Shou D, Zheng R, et al. Moisture and thermal transport properties of different polyester warp-knitted spacer fabric for protective application. *Autex Res J* 2021; 21: 182-191. DOI: 10.2478/aut-2020-0013.
62. Bukhonka NP. Experimental study of structural characteristics, dimensional change in washing, non-creasing properties and air permeability of Swiss double piqué flax knit fabrics. *J Eng Fibers Fabr* 2023; 18: 1-20. DOI: 10.1177/15589250231181701.